energies

MDPI

Article

Optimized Adaptive Overcurrent Protection Using Hybridized Nature-Inspired Algorithm and Clustering in Microgrids

Thiramuni Sisitha Sameera Senarathna * and Kullappu Thantrige Manjula Udayanga Hemapala

Department of Electrical Engineering, University of Moratuwa, Moratuwa 10400, Sri Lanka; udayanga@uom.lk
* Correspondence: sisitha@outlook.com

Received: 15 May 2020; Accepted: 26 June 2020; Published: 30 June 2020

Abstract: Microgrids have been popularized in the past decade because of their ability to add distributed generation into the classic distribution systems. Protection problems are among several other problems that need solutions in order to extract the full capability of these novel networks. This research follows the branches of two major solutions, namely adaptive protection and protection optimization. Adaptive protection implementation with a novel concept of clustering is considered, and protection setting optimization is done using a novel hybrid nature-inspired algorithm. Adaptive protection is utilized to cope with the topology variations, while optimization techniques are used to calculate the protection settings that provide faster fault clearances in coordination with backup protection. A modified IEEE 14 bus system is used as the test system. Validation was done for the fault clearing performance. The selected algorithm was effective than most other algorithms, and the clustering approach for adaptive overcurrent protection was able to reduce the number of relays' setting groups.

Keywords: adaptive protection; microgrid protection; protection optimization; directional overcurrent protection; nature inspired optimization algorithm; k-means clustering

1. Introduction

1.1. Microgrid Protection Challenges

The microgrids have accumulated a considerable amount of interest within the past years and turn out to be an indispensable asset in the power industry. The capability to incorporate renewable power generation into the distribution system is one of the vital reasons for microgrids recognition. A broad array of distributed generation (DG) technologies such as sustainable micro-turbine generation, including wind generation, photovoltaic generation, and energy storage systems, make the microgrid more feasible in both islanded and grid-connected modes [1].

There are several technical disputes to be confronted when trying to access the entire potential of microgrids, and protection is one of those challenging areas [2]. Many solutions were presented, influenced by the improvement of protection techniques. Microgrids containing DG can cause variations in short circuit levels, which is one of the main reasons for these protection challenges. The ability of microgrids to operate islanded of the main utility can make these variations more drastic. Also, the existence of different operating topologies makes the protection selectivity more complicated.

The existence of DG and different operating topologies mainly causes the technical challenges that microgrids face. Protection challenges can be identified as a major area that requires specialized solutions in order to manage efficient running microgrids. A few of the main protection challenges can be identified as follows.

Short-circuit capacity variation due to utility grid connection and disconnection needs to be addressed by changing the relay threshold values accordingly [3]. Microgrid DG penetration can introduce bi-directional power flow which will also cause the fault current to change its direction. They can create protection problems such as unnecessary tripping, relay under reach, and relay overreach [4]. The protection scheme needs to account for the above grid condition changes in order to provide reliable protection against faults.

1.2. Literature Review

The above-mentioned protection challenges need to be addressed to provide a complete microgrid protection solution. The effect of varying short circuit levels by the varying topology can be handled by several methods, including adaptive protection. Differential protection, phasor current-based, phasor voltage-based, and impedance-based are some other solutions. Adaptive protection remains a popular solution among research because of its simplicity. There are also some drawbacks associated with these other schemes. Line differential protection requires reliable communication channels among the protecting equipment and discrete backup protection in case of a communication failure [5]. Current phasor-based methods require aggressive network upgrades, including phasor measurements and communication channels [6]. Voltage phasor-based methods also require rigorous data acquisition and can misoperate during voltage disturbances [7]. A key obstacle to the adaptive scheme is that it requires prior knowledge of all possible configurations. However, when applied to a microgrid, it is not a major issue as the system is relatively small, and the different topologies can be easily handled.

Adaptive protection is defined as an online process of protection response modification in accordance with the network conditions [8]. An adaptive protection system design consists of a set of digital relays, a smart control system that monitors and responds to the network events, and communication infrastructure for the data transfer between processing and actuating pairs. There are several communication-less protection methods proposed in the literature but with less feasibility in the modern meshed type microgrids [9].

The following can be identified as the primary conditions to be satisfied for the practical execution of an adaptive protection scheme. The network should be equipped with digital relays that accept a wide range of tripping attributes, and the switching of these settings should be possible via remote communication. The communication protocol should be compatible with standards such as IEC 61850-3 [10].

One can either use offline analysis and have a set of pre-calculated relay settings applicable to the identified operating mode or revise the relay settings online according to the present topology. In the offline method, a set of profound network topologies must be identified, and the respective protection settings for each state are recalled through an event table. Online calculation for an adaptive protection system is triggered by interruptions on distributed generations [11]. The above research did not take line contingencies into account when identifying the fault current variations. If those other network variations were included, it would be difficult to distinguish each topology accurately using the same method presented.

There are several adaptive protection schemes proposed. Ustun et al. [12] proposed a scheme that updates the relay settings based on the topology of operation. This method only included utility connection and DG connection contingencies. Researchers have been using fuzzy-based systems to identify faults in microgrids [13]. Voltage and current phasor measurements are fed into the fuzzy inference systems to identify the faults. These methods are mainly used for fault identification and classification, where a separate system is required for fault clearance. More advanced artificial neural networks (ANNs) have been used for fault classification in adaptive scenarios of microgrids [14]. This method requires extensive processing to obtain the results, and the researchers have only presented the scheme in an algorithmic state.

Coordination of directional overcurrent relay becomes a critical issue in the meshed systems with distributed energy resources (i.e., microgrids). This challenge has been confronted as early as 1988 [15].

Researchers were eager to find the ideal technique of getting protection relay settings. As the popularity of microgrids grew, which are inheritably multi-sourced and multi-loop in nature, the importance in the coordinated protection settings has also increased.

Different methods, including trial and error and topological analysis, have been used throughout the years [16]. The present interest is mainly on computational intelligence-based optimization techniques. Computational intelligence (CI) methods have become the present interest in many fields of research. There are three main categories of CI as ANN, fuzzy systems, and evolutionary computation. Protection optimization is mainly done using evolutionary computation or nature-inspired algorithms (NIA) that are specialized in solving optimization problems [17]. Some of the benefits can be listed as simplicity, flexibility, derivative-free mechanism, and local optimum avoidance [18].

When considering the researches on microgrid protection optimization, initial attempts were mainly focused on maintaining the coordination between primary and backup relays by installing localized fault current limiters (FCL) [19]. The proceeding researches performed optimization only considering the relays but with linear problem formulations [20]. The algorithms used were also more primitive ones, such as the genetic algorithm (GA). Further improved solutions were proposed by literature, including non-linear optimization and improved algorithms [21]. Nevertheless, these algorithms were still low-performing compared to the more recently introduced algorithms, and the existence of different topologies was not considered. Researchers have studied the possibility of having a common protection setting that is applicable to both grid-connected and islanded modes by including FCLs [22]. This method cannot yield optimum fault-clearing performance, as it makes compromises to work in both operating modes. Authors of [23] considered different DG penetration levels with a radial type network using gravitational search algorithm (GSA). Authors of [24] used non-standard protection curves, and the curve parameters were included in the optimization problem. Even though they used a novel algorithm, the comparison was done only with particle swarm optimization (PSO). They also did not consider different topologies.

Most of the literature did not consider multiple topologies. Consideration of topology clustering for protection optimization was not considered by any previous authors. Protection optimization was mainly applied in a linear formulation, which considers only a single variable. The proposed method covers all the areas, namely considering multiple topologies, performing non-linear optimization, using a novel hybrid optimization algorithm, and utilizing topology clusters.

1.3. Methodology and Paper Structure

This paper proposes a novel protection scheme for microgrids inspired by adaptive protection and optimization techniques. Section 2 describes the introduction of directional overcurrent protection and different variations of adaptive protection implementations. Furthermore, the clustering methods are proposed to group similar topologies together to reduce the complexity of the adaptive settings. Then the protection coordination using optimization algorithms is introduced, and initial stages of problem formulation are presented. In Section 3, the system model used in the simulation is presented. Initial data for the optimization problem are also presented along with the objective function formulation and constraint formulation. Then the selected algorithm and topology clustering method is introduced. In Section 4, simulation results are presented and discussed. Section 5 elaborates on the conclusion and other prominent research achievements, followed by recommendations for future improvements.

2. Adaptive Protection with Relay Coordination

2.1. Overcurrent Protection

Protection of the distribution level networks, including microgrids, are usually handled through four types of relays. These four types can be identified as overcurrent, distance, voltage based, and differential relays. This research is mainly focused on distribution line protection. Overcurrent

and distance are the most commonly used types for line protection. Out of these two, the overcurrent solution is more straightforward and cost-efficient. Even though it is the plainest option, it is more challenging to achieve the protection of novel distribution networks with varying topologies and embedded generation.

Because of the meshed structure and the presence of DG in these networks, directional over current relays (DOCR) are utilized more commonly. This directionality function is extremely important in a meshed system to correctly discriminate the origin of faults. Relays will not operate for fault currents in the "reverse" direction.

The operation of an overcurrent relay is governed by its characteristic curve. The inverse time curve is the widely used type where the operating time is increasing with the magnitude of the fault current. The operating time of a relay can be expressed by Equation (1), with several relay parameters and fault current according to IEC 60255 standard [25]. These parameters are listed in Tables 1 and 2.

$$t = \left[\frac{K_1}{\left(I_f / (PS \times CT_r) \right)^{K_3} - 1} + K_2 \right] \times TDS \tag{1}$$

Table 1. Parameters of overcurrent protection function.

Symbol	Parameter
t	Operating time
TDSTDS	Time dial setting
If	Fault current
PS	Pickup setting
CTr	Current transformer ratio

Table 2. Standard curve parameters for inverse time overcurrent protection.

Standard	Curve Type	K_1	K_2	K_3
ANSI/IEEE	MI—moderately inverse	0.0515	0.1140	0.02
	VI—very inverse	19.61	0.491	2.0
	EI—extremely inverse	28.2	0.1217	2.0
	NI—normally inverse	5.95	0.18	2.0
	STI—short-time inverse	0.02394	0.01694	0.02
IEC-60255	SI—standard inverse	0.14	0	0.02
	VI—very inverse	13.5	0	1
	EI—extremely inverse	80	0	2
	STI—short-time inverse	0.05	0	0.04
	LTI—long-time inverse	120	0	1

2.2. Adaptive Overcurrent Protection

In this paper, adaptive overcurrent protection is implemented with an offline calculation of protection settings. These pre-calculated relay settings are applied according to the operating mode. A set of profound network topologies must be identified, and the respective protection settings for each state are recalled through an event table.

Operating topologies can be identified by considering single contingencies. Each line, generator, and transformer can be disconnected one at a time to obtain new topologies. While it is possible to identify more meaningful topologies by using double contingency, the obtained topologies are sufficient for validating the proposed design.

Clustering of Topologies

In convention, there is the same number of protection setting groups as the number of identified operating topologies. By clustering a similar set of topologies together, they can be operated using the same protection setting group. This effectively reduces the number of protection setting groups to be stored in the earlier mentioned event table.

Clustering is a phenomenon used in data science to group similar data objects. It is primarily a search function that is used to identify similar and dissimilar objects and group them accordingly [26]. Data clustering is vastly utilized in the fields of data mining and pattern recognition. There are several methods to develop clusters, such as hierarchical methods, partition methods, grid-based methods, model-based methods, etc. The k-means clustering algorithm is a widely used method used for data clustering. The main objective of this algorithm is to minimize the distance from each data point to the center of its cluster. Figure 1 illustrates the basic flowchart of the k-means algorithm.

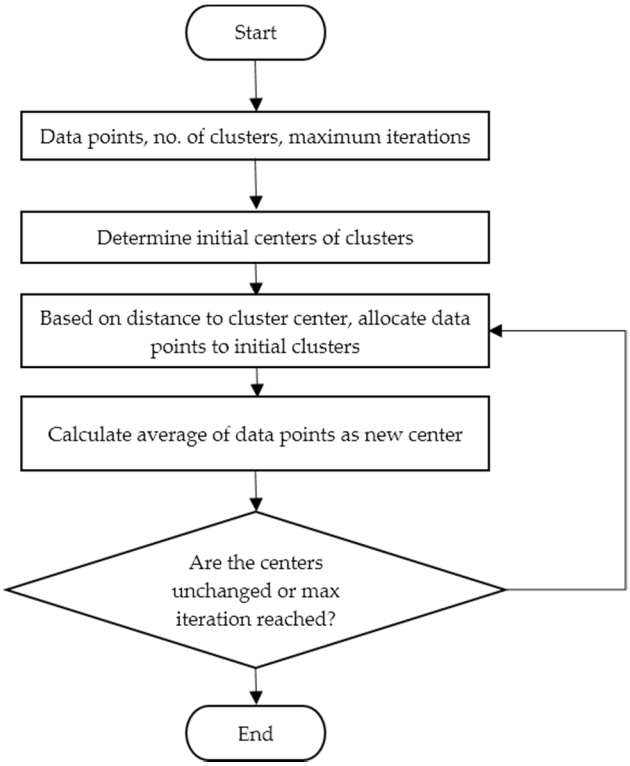

Figure 1. Flowchart of the k-means clustering algorithm.

Initially, the data points, number of desired clusters, maximum iterations, and stating points of centers are determined. Then the distances from every single data point to the closest center is calculated from Equation (2). D_{ij} is the distance between datapoint x and initial center point c, where d is the number of dimensions in the selected space. After calculating the distances, the average of data in the whole cluster is calculated by Equation (3). Here m is the dimension, j is the cluster no, n is the number of data points in the cluster.

$$D_{ij} = \left[\sum_{m=1}^{d} \left(x_{im} - c_{jm}\right)^2\right]^{\frac{1}{2}} \tag{2}$$

$$a_{jm} = \frac{1}{n_j} \sum_{i=1}^{n_j} x_{im} \; ; \; m = 1, 2, \ldots d \tag{3}$$

After that, the new averages are assigned as centers, and the process is repeated until the desired iterations, or there is no considerable change in centers between iterations.

2.3. Protection Coordination with Optimization

Overcurrent relay coordination is done by converting it into an optimization problem. As per the conventional structure of an optimization problem, it includes an objective function, a set of constraints, and the algorithm that is used to generate the solution. The minimization approach is used as the problem is handling time quantities, and operational times should be minimum for an optimal solution.

2.3.1. Different Objective Functions

The sum of relay operating times for a defined fault is the most widespread objective function (OF) utilized by the literature Equation (4) [27–29]. The probability coefficient (w) is used to represent each fault occurrence probability.

$$min\ Z = \sum_{i=1}^{N} w_i t_i \tag{4}$$

The probability coefficient w is typically set as 1, which forces all faults to exhibit an equal rate of occurring. The reflecting three-phase to ground fault for each primary protection zone can either be a near-bus fault Equation (5) [30,31], or both near-bus and far-bus faults Equation (6) [32,33].

$$min\ Z_1 = \sum_{i=1}^{N} t_{i,\ near} \tag{5}$$

$$min\ Z_2 = \sum_{i=1}^{N_{near}} t_{i,\ near} + \sum_{j=1}^{N_{far}} t_{j,\ far} \tag{6}$$

A fault occurring at the beginning of a line near the relay is considered a near-end fault. This near end fault has the maximum short circuit current level for the considered relay. A far-end fault provides the minimum short circuit value for the considered relay while occurring at the furthest end of the line. Operating time for each near-bus fault and far-bus fault can be denoted as $t_{(i,near)}$ and $t_{(j,far)}$, respectively. When both near-bus and far-bus faults are included in the OF, the optimization is expected to become more generalized.

The third type of common OF is the sum of squares of the relay operating times, as in Equation (7) [34,35]. This is mainly used to minimize the backup relay operating times while prioritizing the primary operating times with the squares. The coordination time interval (CTI) constraints are included within the OF second summation term. Here Δt_j is for the relay coordination as in Equation (8). The first term can be used alone for primary relay settings with coordination term included in the constraints as in Equation (9).

$$min\ Z_3 = \sum_{i=1}^{N} (t_i)^2 + \sum_{j=1}^{M} \left(\Delta t_j - \left|\Delta t_j\right|\right)^2 \tag{7}$$

$$\Delta t_j = t_{j,k} - t_{i,k} - CTI \tag{8}$$

$$min\ Z_3 = \sum_{i=1}^{N} (t_i)^2 \tag{9}$$

It was found that these different objective functions do not make a considerable impact on the final results [36]. Therefore, the popular choice of using near-bus fault Equation (5) was used in the proposed scheme.

2.3.2. Optimization Algorithms and Constraint Handling

A large number of optimization algorithms have been used in relay coordination throughout the years. Different optimization algorithms can produce different optimized datasets as output values. Better the algorithm performance, the more optimal the results will be. To identify the degree of optimization for a problem, its OF value can be used as a performance indicator. Hybrid NIA can be identified as a novel type of algorithms that combines two or more primary algorithms. They tend to perform well in obtaining the best optimal solution when compared with other algorithms. The proposed scheme utilizes a hybrid algorithm to get a better solution set.

The algorithms are used in both linear and non-linear problem formulation. In linear scenarios, only a single variable is considered in the optimization, usually the time dial setting (TDS). In these types of linear cases, the other variables, namely pick-up setting (PS) and the curve type are pre-selected using either conventional methods or previous experiences [37]. In non-linear formulation, multiple variables can be included in the optimization. Usually, both TDS and PS are optimized simultaneously [38]. The proposed scheme uses a non-linear optimization formulation.

Multi-objective optimization (MOO) is required when there are multiple objectives to be improved. The relay coordination problem is a multi-objective problem as there are multiple relays to be considered. When performing a MOO simultaneously, compromises are being made in order to achieve the optimal set of solutions. This set of solutions is called the Pareto front. In attaining the required Pareto front solution, there are two popular methods as multi-objective decision-making (MODM) practices and multi-objective optimization techniques.

When using the MODM method, the multi-objective problem is converted into a single objective model, usually through the weighted sum method [39]. Different weights are assigned according to the importance of the objective and added together to formulate a single objective function. At each run of the optimization algorithm, it will provide a solution from its respective Pareto optimal solution set.

The multi-objective optimization technique utilizes a particular multi-objective version of the metaheuristic algorithm. Most of the novel optimization algorithms have their own multi-objective version proposed by the literature. This method is not widely used because of its long execution times and more extensive standard deviation of the solution vector. They usually exhibit weaker algorithm performance when compared with their single objective counterpart [40]. The proposed scheme uses MODM with a weighted sum method.

When solving an optimization problem, there can be constraints that limit the feasible solution space. The constraints should not be violated for a feasible solution. There are two main types of constraints as equality constraints and inequality constraints.

For the above optimization of function Z Equation (4), there are q number of inequality constraints $g(x)$ Equation (10) and m number of equality constraints $h(x)$ Equation (11). Optimization algorithms handle constraints in diverse ways. Some algorithms have inherited constraint handling, where it only requires defining the equality and inequality constraint functions. For example, the GA can perform constrained optimization without any modification of the usual input syntax. Some algorithms cannot process constrained optimization problems and need to use modifications in input data to obtain a feasible solution set, i.e., PSO. The selected algorithm has inherited constraint handling capability, which enables fewer constraint violations than using the penalty method.

$$g_i(x) \leq 0 \; i = 1, \ldots, q \tag{10}$$

$$h_j(x) = 0 \; j = 1, \ldots, m \tag{11}$$

3. Problem Formulation and Simulation

The modified IEEE 14 bus system was considered as the microgrid under testing. Different topologies are identified, and fault current and load flow data for each topology has been obtained.

The optimization problem is then formulated and solved in order to obtain protection settings for each operating topology.

3.1. Modified IEEE 14-Bus System

The 33 kV Distribution section of the IEEE 14 bus system was used as the test model to verify the protection solution. As shown in Figure 2, the 33 kV section is connected with a high voltage section through transformers from bus 6 and bus 9. When disconnected from these links, the distribution section acts as an islanded microgrid. There is only one synchronous generator connected to bus 6 in the original 33 kV section (Table 3). To increase the DG penetration of the system, two similar generators were added to bus 13 and bus 9. Network line parameters and general load parameters are listed in Tables 4 and 5 (Per-unit values are calculated on a 100 MVA base). Complete system parameters can be found in [41].

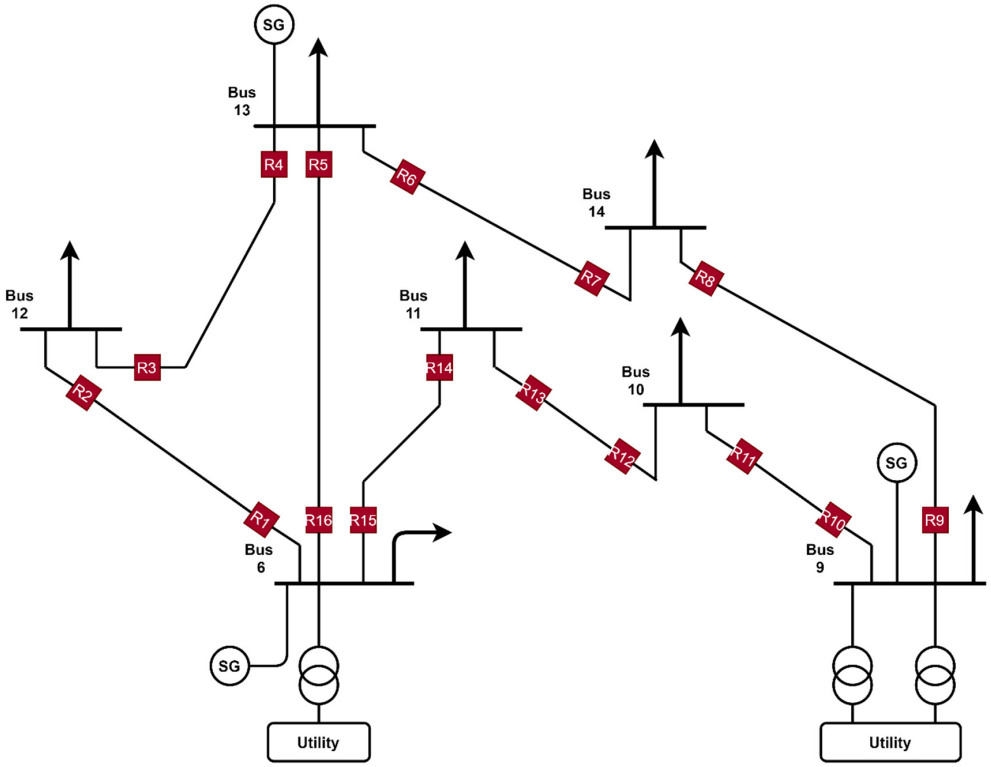

Figure 2. Schematic view of modified 14 bus microgrid.

Table 3. System generator parameters.

Parameter	Value
Connected bus type	PV
Active power	10 MW
Nominal voltage	33 kV
Power factor	0.90
Synchronous reactance (xd)	2 p.u
Synchronous reactance (xq)	2 p.u
Transient reactance (xd')	0.3 p.u
Sub transient reactance (xd'')	0.2 p.u
Stator resistance (rstr)	0.0 p.u
Zero sequence reactance (x0)	0.1 p.u
Zero sequence resistance (r0)	0 p.u
Negative sequence reactance (x2)	0.2 p.u
Negative sequence resistance (r2)	0 p.u
Rotor type	Round rotor

Table 4. System line parameters.

From Bus	To Bus	Line Impedances		Rated Voltage (kV)	Rated Current (kA)
		R (p.u.)	X (p.u.)		
6	12	0.1229	0.2558	33	1
6	13	0.0662	0.1303	33	1
6	11	0.0950	0.1989	33	1
12	13	0.2209	0.1999	33	1
13	14	0.1709	0.3480	33	1
9	14	0.1271	0.2704	33	1
9	10	0.0318	0.0845	33	1
10	11	0.0821	0.1921	33	1

Table 5. System load parameters.

Bus No.	Active Power (MW)	Reactive Power (MVAR)	Configuration [1]
12	6.1	1.6	3PH-D RL
13	13.5	5.8	3PH-D RL
14	14.9	5	3PH-D RL
9	29.5	16.6	3PH-D RL
10	9	5.8	3PH-D RL
11	3.5	1.8	3PH-D RL
6	11.2	7.5	3PH-D RL

[1] 3PH-D RL-Three-phase, resistive-inductive load in the delta configuration.

Each line is equipped with two DOCRs near each bus, and their operating directions are pointing away from the busses. For a fault in the line, the two relays will operate as primary protection, and respective backup relay can be identified from the adjacent lines while considering the directionality.

Single Element Contingencies

In order to represent the variation of topologies, single element contingencies for the modified 14 bus system were considered. New topologies are obtained by disconnecting each line, generator, and utility connection one at a time (Table 6). Eight topologies are obtained by disconnecting one line at a time. Ninth topology is the one with everything connected. Three more topologies can be obtained by disconnecting each generator and utility connection. Additional topology was obtained by disconnecting all three DGs to incorporate a larger variation in short circuit current levels.

Table 6. System topologies formation.

Topology No.	Disconnected Element	Topology No.	Disconnected Element
1	Line 6–12	8	Line 6–11
2	Line 12–13	9	none
3	Line 13–6	10	Gen—bus 13
4	Line 13–14	11	Gen—bus 9
5	Line 14–9	12	Gen—bus 6
6	Line 9–10	13	Utility
7	Line 10–11	14	All 3 DGs

3.2. Load Flow and Short Circuit Analysis

The above modified 14 bus system is simulated in DigSILENT Powerfactory software (DIgSILENT GmbH, Gomaringen, Germany). Load flow analysis is done for each topology to obtain current flowing through each relay at its nominal operation. During the topology 13, load curtailing was done to balance the generation and demand. Every load value was adjusted by a scale factor of 0.3 only in topology 13. Load flow values are used as lower limits when calculating the pickup settings of the

relays. These values are indicated in Table 7. Current transformer (CT) ratios are also indicated in the table, and all current values in the table are in amperes. Throughout this paper, R is used to denote DOCRs followed by the relevant relay number (e.g., R2, DOCR number 2), and T is used to denote the topology number (e.g., T4, topology number 4 as in Table 6).

Table 7. Load flow analysis for normal operation.

R	Load Flow Current (A)														CT Ratio
	T01	T02	T03	T04	T05	T06	T07	T08	T09	T10	T11	T12	T13	T14	
1	-	103	226	75	132	94	108	112	102	132	106	98	11	132	1500/5
2	-	−103	−226	−75	−132	−94	−108	−112	−102	−132	−106	−98	−11	−132	500/5
3	−105	-	122	−29	27	−11	6	11	−2	27	3	−7	−20	26	500/5
4	105	-	−122	29	−27	11	−6	−11	2	−27	−3	7	20	−26	1500/5
5	−285	−194	-	−87	−306	−166	−220	−240	−195	−306	−212	−177	21	−306	1600/5
6	120	134	63	-	273	97	166	191	134	91	155	110	70	88	1250/5
7	−120	−134	−63	-	−273	−97	−166	−191	−134	−91	−155	−110	−70	−88	600/5
8	−145	−130	−208	−266	-	−173	−106	−85	−130	−179	−114	−157	−13	−190	750/5
9	145	130	208	266	-	173	106	85	130	179	114	157	13	190	1500/5
10	106	110	89	−92	168	-	177	243	110	138	94	145	9	155	2000/5
11	−106	−110	−89	92	−168	-	−177	−243	−110	−138	−94	−145	−9	−155	1000/5
12	−94	−87	−124	−155	−26	−183	-	66	−87	−61	−118	−52	−44	−59	1500/5
13	94	87	124	155	26	183	-	−66	87	61	118	52	44	59	1000/5
14	−155	−148	−185	−215	−80	−249	−64	-	−149	−120	−180	−111	−63	−114	800/5
15	155	148	185	215	80	249	64	-	149	120	180	111	63	114	2000/5
16	285	194	-	87	306	166	220	240	195	306	212	177	−21	306	2000/5

Problem formulation for optimization requires short circuit current values through each relay. Short circuit analysis is done for the test system model, according to IEC60909 [42] because of the presence of distributed generation [43]. Three-phase to ground fault is considered as the maximum short circuit value. Near-bus faults are taken as the maximum fault current value while the far-bus fault current is considered as the minimum.

For the modified 14 bus system, short circuit analysis was done for all selected topologies. All primary backup relay pairs were considered, and both near-bus and far-bus 3 ph fault values were recorded. Table 8 presents the fault analysis for topology no 1.

Table 8. Fault currents through primary and backup relay pairs for topology 1.

Primary R	Backup R	3 ph Near-Bus Fault		3 ph Far-Bus Fault	
		Current Seen by Primary R (kA)	Current Seen by Backup R (kA)	Current Seen by Primary R (kA)	Current Seen by Backup R (kA)
1	5	-	-	-	-
1	14	-	-	-	-
2	4	-	-	-	-
3	1	0.000	0.000	0.000	0.000
4	16	17.707	7.116	4.999	2.009
4	7	17.707	2.200	4.999	0.621
5	3	10.811	0.000	5.864	0.000
5	7	10.811	2.228	5.864	0.873
6	16	15.415	7.051	3.752	1.479
6	3	15.415	0.000	3.752	0.000
7	9	4.805	4.805	2.268	2.268
8	6	3.699	3.699	2.123	2.123
9	11	19.591	2.655	4.891	0.411
10	8	19.378	2.085	10.219	0.983
11	13	3.442	3.442	2.749	2.749
12	10	10.057	10.057	4.753	4.753
13	15	5.923	5.923	3.466	3.466
14	12	4.699	4.699	2.764	2.764
15	5	19.177	5.706	6.006	1.660
15	2	19.177	0.000	6.006	0.000
16	14	16.311	2.710	7.319	0.965
16	2	16.311	0.000	7.319	0.000

3.3. Optimization Algorithm Implementation

Optimization algorithm implementation can be separated into two areas as objective function formulation and constraint formulation. Relay operating time is the principal consideration of the optimization, and the minimization approach is used. Short circuit data and load flow data are used in this formulation while the minimization problem is solved to find the best set of values for the decision variables.

3.3.1. Objective Function Formulation

Objective function formulation can be considered the fundamental stage of the optimization process. As described in Section 2.3.1, the summation of the relay operating times is used to form the objective function. The final goal is to minimize this summation Equation (12), subject to different constraints.

From the Equation (13) for the operating time of a relay, TDS and PS are considered variables. They are called decision variables, and the final solution is to find the optimal set of values for these decision variables. As for the curve type, the IEC standard inverse curve is selected.

$$min\ Z = \sum_{i=1}^{N} f_i \tag{12}$$

$$T = \frac{K_1 \times \boldsymbol{TDS}}{\left(I_f\ /\left(\boldsymbol{I}_{pickup}\right)\right)^{K_2} - 1} \tag{13}$$

Summation of all relay operating times for maximum short circuit currents is taken. Fault current values are substituted from the short circuit analysis, and the time-current curve type was taken as the standard inverse. For minimization, we get a function of TDS and PS Equation (14).

$$\min Z = f\ (TDS_1, TDS_2, \ldots,\ TDS_N,\ PS_1,\ PS_2,\ \ldots,\ PS_N) \tag{14}$$

3.3.2. Constraint Formulation

There are two types of constraints applied in the optimization process to achieve an accurate set of solutions. They are decision variable bounds and functional constraints.

Decision variable bounds are applied to the decision variables according to their physical limitations. TDS values are limited between 0.05 and 1.1 according to relay manufacturer limitations, and PS values are bound between overload currents and minimum fault currents [28,30,44] (Equations (15)–(19)).

$$TDS_i^{min}\ \leq\ TDS_i \leq\ TDS_i^{max} \tag{15}$$

$$0.05 \leq\ TDS_i\ \leq\ 1.1 \tag{16}$$

$$I_{pickup}^{min}\ \leq\ I_{pickup} \leq\ I_{pickup}^{max} \tag{17}$$

$$I_{pickup}^{min} = 1.5 \times I_{load} \tag{18}$$

$$I_{pickup}^{max} = \frac{2}{3} \times I_{\text{fault, } min} \tag{19}$$

Functional constraints are used to keep the coordination between primary and backup relays. The operation time difference between a primary relay and a backup relay is set to be greater than the CTI Equation (20). CTI value was selected as 0.2 s. Relay operating times are also limited to achieve safe fault clearances as in Equation (21).

$$t_{j,k}\ -\ t_{i,k}\ \geq\ CTI \tag{20}$$

$$0.05 \leq t_{i,op} \leq 1.00 \tag{21}$$

This system has a total of 16 relays; therefore, with two variables per each relay makes the total decision variables to 32. An objective function is formed by taking the summation of maximum fault operating times of each relay. Both decision variable bounds and functional constraints are formulated with the load flow data and short circuit data from Section 3.2. Primary relay operating time limits are also included in the main constraint function.

3.4. WCMFO Algorithm

Hybrid water cycle–moth flame optimization algorithm (WCMFO) is a combination of two primary algorithms, namely the water cycle optimization algorithm and the moth flame optimization algorithm. This algorithm was initially proposed by Khalilpourazari et al. [45].

Water cycle algorithm (WCA) is a novel optimization algorithm inspired by the flow of water streams toward the sea. Figure 3a illustrates a simple schematic of the algorithm composition. This algorithm includes evaporation and raining conditions to provide necessary randomization between iterations. This feature enables the optimization results to avoid local bests and get closer to the global solution.

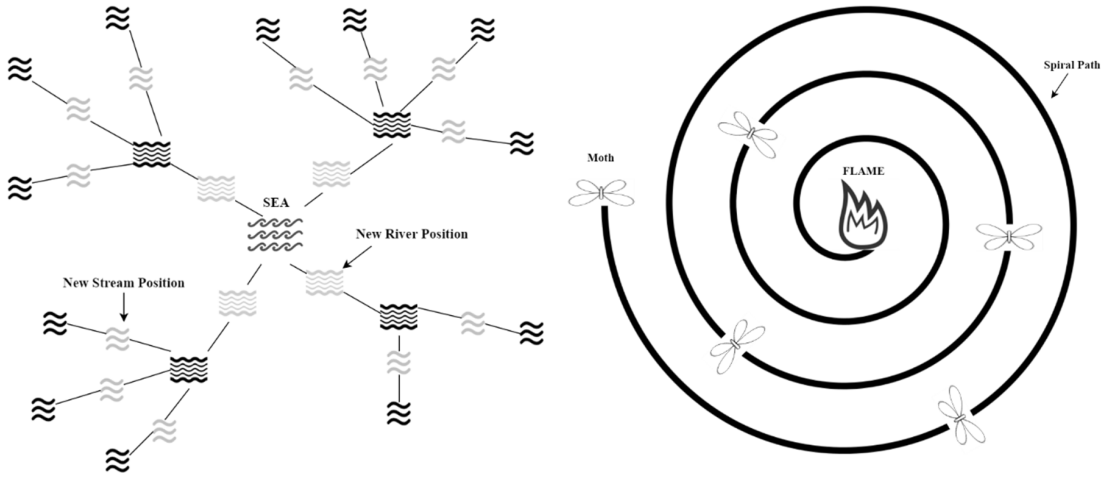

Figure 3. (**a**) Water cycle algorithm (WCA) schematic diagram; (**b**) spiral fly pattern of the moths around a flame.

Moth flame optimization (MFO) algorithm is inspired by the flying patterns of moths around a light source. Figure 3b illustrates the fly patterns used for the algorithm. Each moth represents a solution and flies around their corresponding flame. With each algorithm iteration, the number of flames is reduced to obtain the final solution.

A combination of these algorithms makes a high-performance metaheuristic algorithm. WCA has improved solution space exploration ability constructed on its streams and river formation. MFO has a great ability in exploitation because of the localized formation of flames. WCMFO is designed to combine these advantages of the underlying algorithms. WCA is the base algorithm of the WCMFO hybrid algorithm. The stream positions are then updated according to the spiral movement from the MFO algorithm. WCMFO has an improved raining process to increase the randomization using levy flight.

3.5. Clustering for Adaptive Protection

In the modified IEEE 14 bus system model, optimization was done using the WCMFO algorithm for different operating topologies. Instead of calculating a separate set for every topology, clustering was used to identify similar topologies and they were given the same set of protection settings.

As described in Section 3.1, there are 14 topologies under consideration. Most industrial overcurrent relays have facilities to save at least four setting groups. Here the available 14 topologies are divided into four clusters according to their overall short circuit levels. The number of clusters to be created will depend on the relay's ability and deviation of the topologies.

The deviation of the short circuit current for each relay at every topology is considered the clustering factor. The mean value of each primary relay's maximum fault current was calculated using Equation (22). Here, Ri is the relay number, and $I_{f,\,Ri,\,Tx}$ is the maximum fault current (3-ph near-bus) of relay Ri for the operating topology Tx. $N_{non\text{-}zero}$ is the population size without including zero-current scenarios (e.g., for R1, $N_{non\text{-}zero}$ is 13 without including the T1 scenario where R1 is disconnected). These mean values are presented in Table 9. The sum of deviation of currents for each topology was calculated using Equation (23). Here, Tx is the topology number, and $I_{f,\,Ri,\,Tx}$ is the same as above. Deviation of each relay's maximum fault current from its calculated mean (M_{Ri}) was aggregated for each topology, obtaining the summation of deviations for a given topology. These values are presented in Table 10.

Table 9. Mean value of each relay's maximum fault current.

Ri	M_{Ri} (kA)	Ri	M_{Ri} (kA)	Ri	M_{Ri} (kA)	Ri	M_{Ri} (kA)
1	17.76	5	10.28	9	17.02	13	5.55
2	3.98	6	13.84	10	17.03	14	4.41
3	4.42	7	4.55	11	3.23	15	16.99
4	14.39	8	3.48	12	9.18	16	14.87

Table 10. Sum of deviation in short circuit current (SCC) for each topology.

Tx	S_{Tx} (kA)	Tx	S_{Tx} (kA)
1	−16.21	8	−12.65
2	−16.73	9	−23.62
3	1.60	10	15.77
4	−13.80	11	−0.09
5	−13.66	12	8.98
6	−12.58	13	18.70
7	−14.66	14	78.93

Figure 4 provides the summation of deviations for each topology. Here we can identify four distinct groups. After deciding on the number of clusters, each cluster can be finalized using the k-means algorithm. Topology no 14 is separated into its own cluster, and topologies 1, 2, 4, 5, 6, 7, 8, 9 are grouped into another cluster. The remaining two clusters are selected as topologies 3, 11, and topologies 10, 12, 13. Table 11 presents the grouping of topologies into clusters.

$$M_{Ri} = \frac{\sum_{x=1}^{14} I_{\,f,\,Ri,\,Tx}}{N_{non-zero}} \tag{22}$$

$$S_{Tx} = \sum_{i=1}^{16} (M_{Ri} - I_{f,\,Ri,\,Tx}) \tag{23}$$

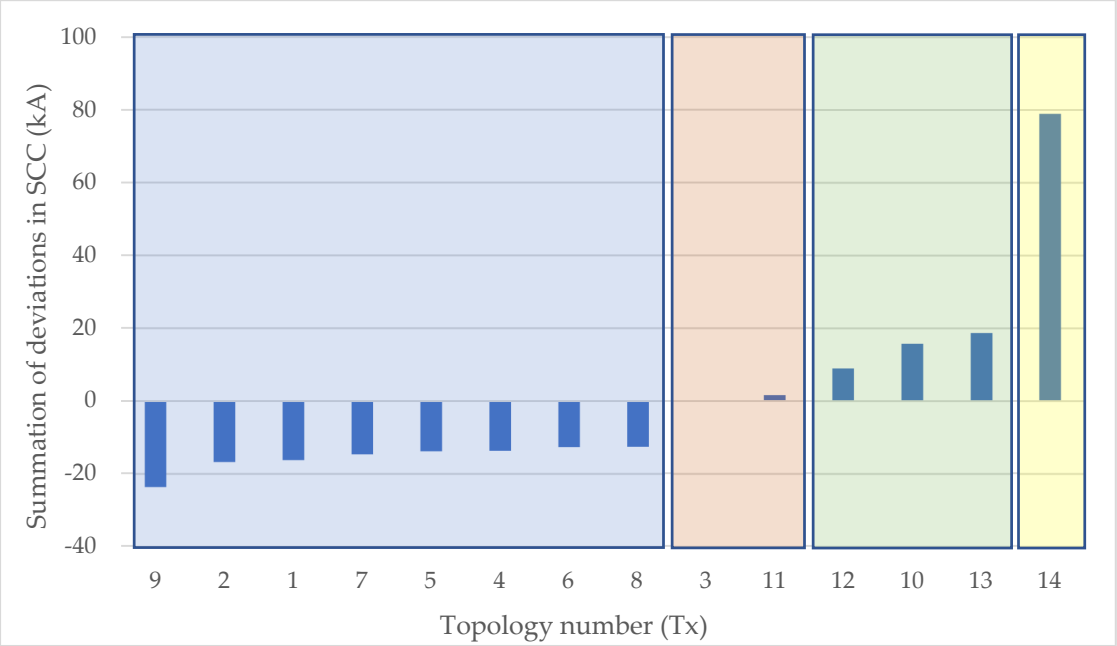

Figure 4. Variation of short circuit level deviation of topologies.

Table 11. Topologies divided into clusters.

Cluster 1	Cluster 2	Cluster 3	Cluster 4
Topology 1 Topology 2 Topology 4 Topology 5 Topology 6 Topology 7 Topology 8 Topology 9	Topology 3 Topology 11	Topology 10 Topology 12 Topology 13	Topology 14

The objective function was formed with the maximum currents of the set of topologies belonging to the relevant cluster. When imposing constraints, some topologies had similar constraints, which had to be put only once effectively reducing the number of constraints. Minimum and maximum operating times constraints were also imposed for the minimum and maximum fault values considering the whole cluster. Decision variable bounds were set considering all the values ranging throughout the cluster.

4. Results and Discussion

Optimization is run on MATLAB software to obtain the best data set for the decision variables. These obtained relay settings are then put into the Equations, and the validity of operating time for the faults are observed. The settings are further applied to the DigSILENT simulation model, and relay time-current curves are also obtained.

Several popular algorithms were used to compare the performance of the WCMFO algorithm. These algorithms and corresponding references are presented in Table 12. The cluster 3 data were used for the comparison calculation. Obtained protection settings and OF values of each algorithm are depicted in Table 13. It is evident that WCMFO has the lowest OF value of all comparing algorithms. OF value can be identified as the total operating time of relays, and the net gain in operating time is compared in Table 14. This is about a 54% decrease in total relay operating time from the worst solution which is the PSO data set. It is a 5.3% decrease from the second-best solution obtained through GWO.

Table 12. Optimization algorithms used for comparison.

Algorithm	References	
	Algorithm	**Application**
Modified Particle Swarm Optimization (PSO)	K. Masuda, 2010. [46]	M.M Mansour, 2007. [47]
Particle Swarm Optimization-Gravitational Search Algorithm (PSOGSA)	S. Z. M. Hashim, 2010. [48]	A. Srivastava, 2016. [49]
Harris Hawks Optimization (HHO)	A.A Heidari, 2019. [50]	J. Yu, 2020. [51]
Whale Optimization Algorithm (WOA)	S. Mirjalili, 2016. [52]	A. Wadood, 2019. [27]
Grey Wolf Algorithm (GWO)	A. Lewis, 2014. [53]	A. Korashy, 2018. [54]
Water Cycle—Moth Flame Algorithm (WCMFO)	S. Khalilpourazari, 2019. [45]	-

Table 13. Time dial setting (TDS) and pick-up setting (PS) by different algorithms compared against objective function value.

R	PSO		PSOGSA		HHO		WOA		GWO		WCMFO	
	TDS (s)	PS (A)	TDS (s)	PS (A)	TDS (s)	PS (A)	TDS (s)	PS (A)	TDS (s)	PS (A)	TDS (s)	PS (A)
1	0.18	3.45	0.05	9.02	0.20	1.58	0.18	2.39	0.14	3.89	0.14	3.86
2	0.36	1.47	0.18	1.01	0.21	1.11	0.22	1.00	0.21	1.00	0.16	1.33
3	0.40	1.52	0.15	1.10	0.20	2.02	0.24	2.02	0.24	2.02	0.25	1.96
4	0.66	1.54	0.05	7.07	0.19	1.30	0.19	1.35	0.19	1.33	0.18	1.30
5	0.14	2.34	0.25	1.16	0.21	1.15	0.23	1.00	0.22	1.00	0.22	1.00
6	0.44	5.14	0.24	2.02	0.19	2.34	0.18	2.40	0.09	6.28	0.11	5.65
7	0.23	3.57	0.26	1.00	0.20	2.44	0.25	1.96	0.24	2.28	0.22	2.93
8	0.41	3.11	0.14	1.79	0.20	1.99	0.21	1.89	0.15	3.57	0.20	2.43
9	0.21	4.53	0.28	1.00	0.20	2.32	0.19	2.62	0.22	2.21	0.10	6.43
10	0.27	5.03	0.11	5.95	0.20	2.58	0.20	2.51	0.11	7.22	0.12	6.38
11	0.28	2.91	0.05	7.48	0.20	2.84	0.14	2.84	0.14	3.30	0.12	3.37
12	0.30	5.41	0.39	1.09	0.20	2.20	0.15	3.37	0.10	6.50	0.10	5.94
13	0.16	7.86	0.34	3.30	0.20	3.39	0.15	3.73	0.06	9.89	0.05	9.89
14	0.32	4.57	0.45	1.00	0.20	2.38	0.19	2.31	0.25	1.99	0.18	3.25
15	0.10	6.38	0.53	1.82	0.20	2.12	0.17	2.28	0.09	4.49	0.06	6.51
16	0.42	4.05	0.39	1.52	0.20	1.59	0.18	1.87	0.10	5.11	0.10	5.11
OF	16.8236 s		10.0170 s		8.6590 s		8.2953 s		8.1858 s		7.7457 s	

Table 14. Comparison of the total net gain from water cycle–moth flame optimization (WCMFO) algorithm.

Comparing Algorithms	The Net Gain in Total Operating Time (s)	Percentage Gain (%)
WCMFO/PSO	9.0779	53.96
WCMFO/PSOGSA	2.2713	22.67
WCMFO/HHO	0.9133	10.55
WCMFO/WOA	0.5496	6.63
WCMFO/GWO	0.4401	5.38

When comparing the computational burden of each algorithm, PSOGSA and HHO took the least central processing unit (CPU) time to converge into a solution within 500 and 1000 iterations, respectively. PSO algorithm took 1103 s of CPU time to converge from 8000 iterations. GWO and WOA were executed with 10,000 iteration limits and took 2105 s and 1530 s, respectively. WCMFO

only needed 200 iterations to reach the best solution with 2293 s of CPU time. WCMFO required a smaller number of iterations but needed higher processing time.

WCMFO was used to obtain the protection settings for the rest of the clusters. The full list of relay settings is presented in Table 15. Here PS values are presented as CT secondary current values.

Table 15. Relay settings obtained for each cluster.

R	Cluster 1		Cluster 2		Cluster 3		Cluster 4	
	TDS (s)	PS (A)	TDS (s)	PS (A)	TDS (s)	PS (A)	TDS (s)	PS (A)
1	0.10	5.04	0.10	4.22	0.14	3.86	0.07	3.08
2	0.12	3.53	0.24	1.79	0.16	1.33	0.05	1.91
3	0.22	1.03	0.14	2.66	0.25	1.96	0.06	4.41
4	0.20	1.00	0.14	3.70	0.18	1.30	0.10	1.10
5	0.11	3.36	0.12	3.32	0.22	1.00	0.07	1.82
6	0.05	7.67	0.05	7.53	0.11	5.65	0.07	3.51
7	0.12	4.20	0.15	3.77	0.22	2.93	0.16	3.53
8	0.06	6.09	0.07	6.46	0.20	2.43	0.08	2.38
9	0.08	5.77	0.19	2.13	0.10	6.43	0.13	3.50
10	0.07	9.99	0.08	8.51	0.12	6.38	0.08	5.46
11	0.14	1.53	0.23	1.15	0.12	3.37	0.05	3.87
12	0.05	9.07	0.07	7.33	0.10	5.94	0.06	5.66
13	0.20	1.75	0.32	1.02	0.05	9.89	0.05	5.49
14	0.24	1.03	0.13	2.94	0.18	3.25	0.12	2.71
15	0.06	8.45	0.09	6.85	0.06	6.51	0.12	1.83
16	0.19	1.53	0.20	1.32	0.10	5.11	0.14	1.15
OF	5.3431 s		6.6272 s		7.7457 s		5.0519 s	

Topology 1 relay operating times were obtained by using the settings given by cluster 1 solution. Full relay operating times for each maximum 3 ph fault for every relay is presented in Table 16. Currents through both primary relay and backup relay are listed under the fault current column. Both primary and backup relay operating times are included under the operating time column, and CTIs are calculated. Primary relay operating times does not exceed the operating limits of 1 s or 0.05 s. CTI values also do not fall below 0.2 s minimum limit.

Table 16. Relay operating time and coordination time interval (CTI) of obtained settings for topology 1.

Relay		Fault Current (A)		Operating Time (s)		CTI (s)
Primary R	Backup R	Primary R	Backup R	Primary R	Backup R	
1	5	-	-	-	-	-
1	14	-	-	-	-	-
2	4	-	-	-	-	-
3	1	0	0	-	-	-
4	16	17,707	7116	0.3318	0.5319	0.2001
4	7	17,707	2200	0.3318	0.5535	0.2217
5	3	10,811	0	0.3193	-	-
5	7	10,811	2228	0.3193	0.5487	0.2294
6	16	15,415	7051	0.1644	0.5339	0.3695
6	3	15,415	0	0.1644	-	-
7	9	4805	4805	0.3589	0.5591	0.2003
8	6	3699	3699	0.3165	0.5290	0.2126
9	11	19,591	2655	0.2320	0.4460	0.2140
10	8	19,378	2085	0.2877	0.5393	0.2516
11	13	3442	3442	0.3971	0.6008	0.2037
12	10	10,057	10,057	0.2884	0.4955	0.2070
13	15	5923	5923	0.4830	0.7231	0.2401
14	12	4699	4699	0.4948	0.6951	0.2003
15	5	19,177	5706	0.2308	0.4443	0.2135
15	2	19,177	0	0.2308	-	-
16	14	16,311	2710	0.3942	0.5953	0.2011
16	2	16,311	0	0.3942	-	-

Table 17 presents the fault currents and operating times for the relay pair 4 and 7 throughout the thirteen topologies. Relay 4 is the primary relay for faults between bus 12 and 13, and the corresponding backup relay is relay 7. Fault currents seen by the primary relay from both near-end and far-end faults are considered, and both operating times are within the safe limits. Figure 5a presents the Relay 4 fault current, and Figure 5b depicts the corresponding relay operating times for each topology.

Table 17. Fault current and operating time for different topologies in primary/backup pair R4 and R7.

Topology Number	R4 Current (Primary) (A)		R4 Operating Time (Primary) (s)		R7 Current (Backup) (A)		R7 Operating Time (Backup) (s)	
	Near-Bus Fault	Far-Bus Fault	Near-Bus Fault	Far-Bus Fault	Near-Bus Fault	Far-Bus Fault	Near-Bus Fault	Far-Bus Fault
T1	17,707	4999	0.3318	0.4872	2200	621	0.5535	3.9629
T2	-	-	-	-	-	-	-	-
T3	10,892	4311	0.4196	0.7130	2369	834	0.6236	1.7050
T4	15,091	4263	0.3459	0.5173	0	0	-	-
T5	15,091	4263	0.3459	0.5173	0	0	-	-
T6	16,728	4381	0.3367	0.5119	2299	855	0.5372	1.5587
T7	16,728	4381	0.3367	0.5119	2299	855	0.5372	1.5587
T8	16,728	4381	0.3367	0.5119	2299	855	0.5372	1.5587
T9	17,001	4425	0.3353	0.5099	2171	733	0.5586	2.2033
T10	8659	3183	0.3946	0.5887	2193	1139	0.8159	1.2785
T11	16,495	4368	0.3535	0.7060	1849	591	0.7352	3.9126
T12	14,816	4096	0.3345	0.5242	2070	787	0.8430	1.8709
T13	15,448	4210	0.3306	0.5180	1871	661	0.8948	2.3909
T14	5633	2313	0.2346	0.3449	1694	1053	0.8037	1.2296

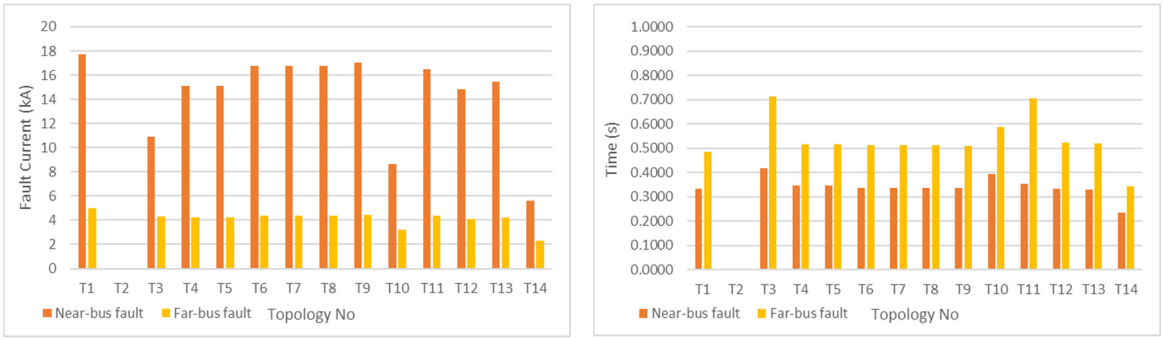

(**a**) (**b**)

Figure 5. (**a**) Current seen by primary R4 for both near-end and far-end faults; (**b**) R4 primary operating times for both near-end and far-end faults.

Figure 6a presents fault currents seen by the backup relay R7, and Figure 6b illustrates the relevant operating times for every topology. Even though the backup relay operating times were not limited to 1 s constraints, they are within acceptable limits and follow perfect coordination. Table 18 depicts the CTI values for both near-end faults and far-end fault.

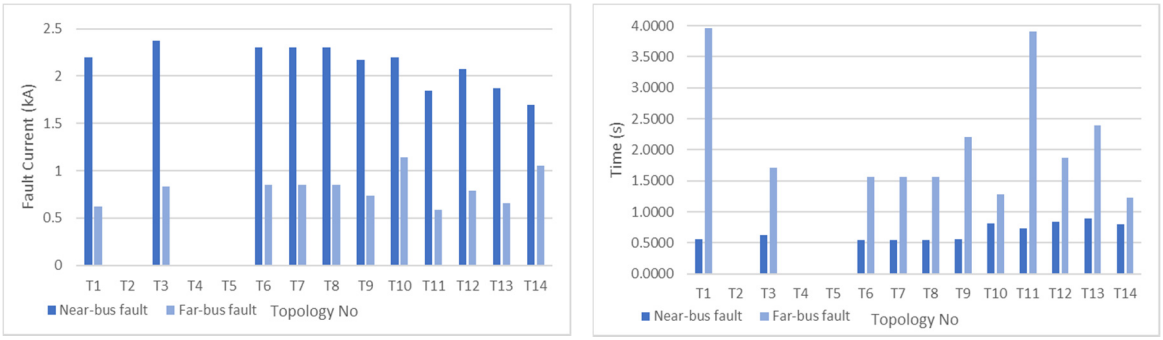

(**a**) (**b**)

Figure 6. (**a**) Current seen by backup R7 for both near-end and far-end faults; (**b**) R7 backup operating.

Table 18. Relay 4 and 7 pair CTI variation for different topologies.

Topology Number	CTI (s)	
	Near-Bus Fault	Far-Bus Fault
T1	0.22	3.48
T2		
T3	0.20	0.99
T4	-	-
T5	-	-
T6	0.20	1.05
T7	0.20	1.05
T8	0.20	1.05
T9	0.22	1.69
T10	0.42	0.69
T11	0.38	3.21
T12	0.51	1.35
T13	0.56	1.87
T14	0.57	0.88

The following graphs (Figures 7–10) were obtained by feeding the optimized settings back to the DigSILENT model. Three-phase to ground fault was made at the middle of the line (50%-line length), and relay operation curves were obtained. Relay current values are represented in the *x*-axis in amperes, and the *y*-axis is time in seconds with log scaling. The red curve represents the primary relay time-current curve, and the respective current seen by the primary relay is represented in the red vertical line. Operating time for this primary operation is at the intersection point. Green curves are backup relay curves, and when there is more than one backup relay, the blue curve also represents the backup curve. If the fault current seen by the backup relay is different from the fault current seen by the primary relay, they are represented in vertical lines of relevant color, and their intersection points are the relevant operating times.

Figure 7a presents the R1, R5, and R14 characteristics and currents through each relay when a fault occurs within the primary protection area of R1 (the line from bus 12 to bus 6). A fault is created at 50% of line length, and the considered topology is T2. Here R5 and R14 operate as backup protection according to their own characteristics and fault currents. Figure 7b presents the curves for R4, R7, and R16 and currents through each relay when a fault occurs within the primary protection area of R4 (the line from bus 12 to bus 13). A fault is created at the midpoint of the line as previously, and the considered topology is T9. Here R7 and R16 operate as backup protection according to their own characteristics and fault currents. Similarly, Figure 8a shows the same fault scenario for R7 and R9, where the topology is T3, and the primary relay is R7. Figure 8b shows the fault scenario for R15, R5,

and R2, where the topology is T11, and the primary relay is R15. Similarly, Figures 9 and 10 present characteristic curves and similar fault scenarios for T10, T13, and T14.

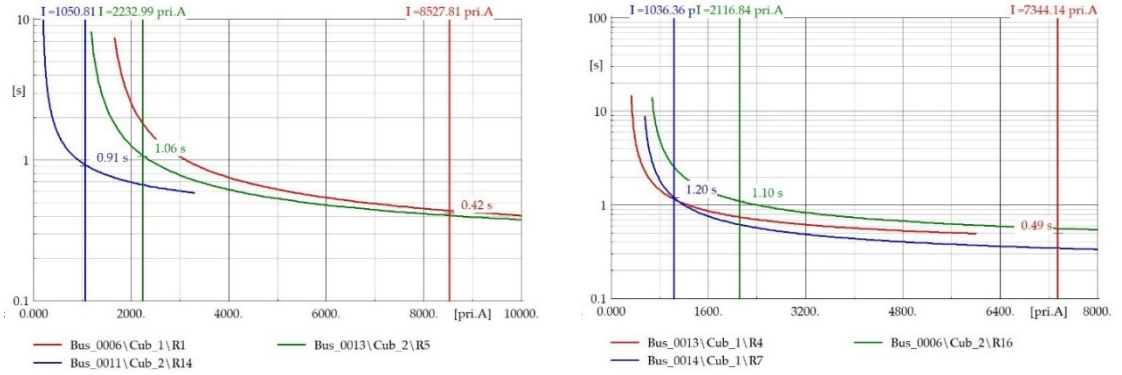

(**a**) (**b**)

Figure 7. (**a**) T2, R1 (red) primary operation with backup R5 (green) and R14 (blue) obtained with cluster 1 settings; (**b**) T9, R4 (red) primary operation with backup R16 (green) and R7 (blue) obtained with cluster 1 settings.

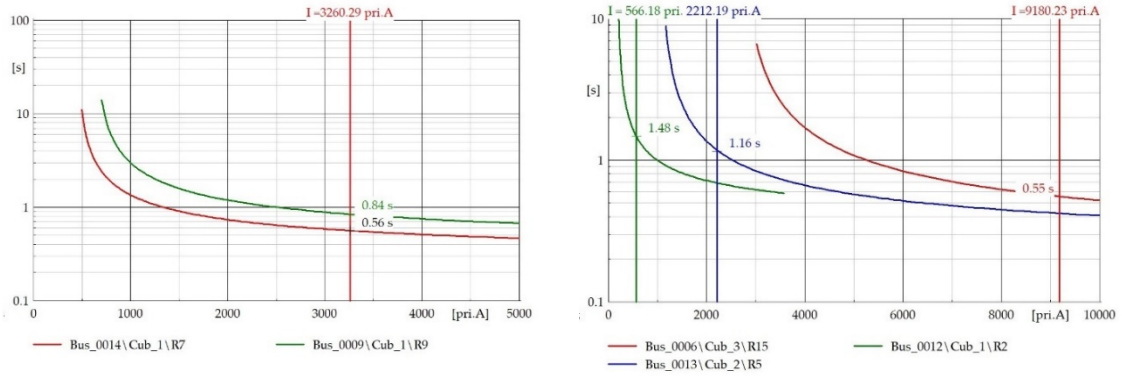

(**a**) (**b**)

Figure 8. (**a**) T3, R7 (red) primary operation with backup R9 (green) obtained with cluster 2 settings; (**b**) T11, R15 (red) primary operation with backup R5 (blue) and R2 (green) obtained with cluster 2 settings.

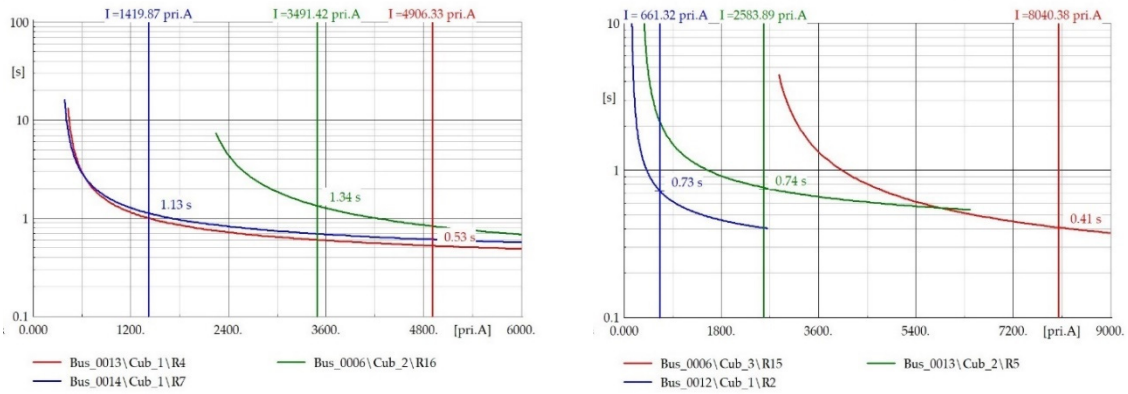

(**a**) (**b**)

Figure 9. (**a**) T10, R4 (red) primary operation with backup R16 (green) and R7 (blue) obtained with cluster 3 settings; (**b**) T13, R15 (red) primary operation with backup R5 (green) and R2 (blue) obtained with cluster 3 settings.

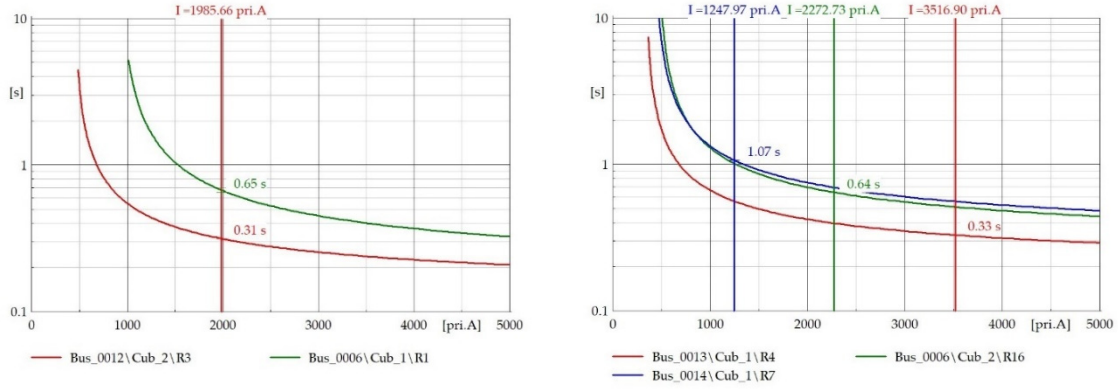

(**a**) (**b**)

Figure 10. (**a**) T 14, R3 (red) primary operation with backup R1 (green) obtained with cluster 4 settings; (**b**) T14, R4 (red) primary operation with backup R16 (green) and R7 (blue) obtained with cluster 4 settings.

It is evident that the settings group for each cluster is valid for all topologies belonging to that cluster. This clustering approach vastly reduces the number of adaptive stages while grouping similar topologies.

5. Conclusions

This paper focused on two principal areas of microgrid protection as the existence of multiple operating modes and the difficulty of relay coordination due to the multi-sourced and multi-loop network architecture. Identified solutions were the use of adaptive protection and using a computational intelligence-based relay setting optimization method. The clustering method was used in handling the different adaptive scenarios. Network element single contingencies were used to define operating topologies. Clustering was used to group similar topologies together in terms of the short circuit current. It proved to be effective in reducing the number of effective protection settings groups needed for the correct operation of the protection system.

A novel hybrid algorithm was used in obtaining the optimized protection settings. WCMFO algorithm confirmed its superiority among the other algorithms, such as GWO, WOA, HHO, PSOGSA, and PSO. As these are some of the better-performing novel algorithms, it is safe to assume WCMFO is better than most of the algorithms. However, there is always a possibility of a better-performing algorithm with a different hybrid combination. The proposed method has a 50% to 5% decrease in the total relay operating time among the results obtained through other algorithms. Final relay operating times obtained by the settings were well within the initialized constraints. Coordination times did not go below the 0.2 s margin, and the fault operating times did not exceed 1 s for the primary protection. This research presents the successful implementation of adaptive protection using metaheuristics and clustering. This method limited itself to a single type of standard time–current curve, and the selected topologies were based on single element contingencies. Exploring these areas can be identified as future research directions for a flexible protection solution.

Author Contributions: Conceptualization, T.S.S.S. and K.T.M.U.H.; methodology, T.S.S.S.; software, T.S.S.S.; validation, T.S.S.S. and K.T.M.U.H.; formal analysis, T.S.S.S.; investigation, T.S.S.S.; resources, T.S.S.S. and K.T.M.U.H.; data curation, T.S.S.S.; writing—original draft preparation, T.S.S.S. and K.T.M.U.H.; writing—review and editing, T.S.S.S. and K.T.M.U.H.; visualization, T.S.S.S.; supervision, K.T.M.U.H.; project administration, K.T.M.U.H.; funding acquisition, K.T.M.U.H. All authors have read and agreed to the published version of the manuscript.

Funding: This research was funded by National Research Council Sri Lanka, grant number 17-065.

Acknowledgments: The authors gratefully acknowledge the support from the University of Moratuwa throughout the research.

Conflicts of Interest: The authors declare no conflict of interest. The funders had no role in the design of the study; in the collection, analyses, or interpretation of data; in the writing of the manuscript, or in the decision to publish the results.

References

1. Tanrioven, M. Reliability and cost–benefits of adding alternate power sources to an independent micro-grid community. *J. Power Sources* **2005**, *150*, 136–149. [CrossRef]
2. Senarathna, T.S.S.; Udayanga Hemapala, K.T.M. Department of Electrical Engineering, University of Moratuwa, Moratuwa, Sri Lanka Review of adaptive protection methods for microgrids. *AIMS Energy* **2019**, *7*, 557–578. [CrossRef]
3. Maqbool, U.; Khan, U.A. Fault current analysis for grid-connected and Islanded Microgrid modes. In Proceedings of the 2017 13th International Conference on Emerging Technologies (ICET), Islamabad, Pakistan, 27–28 December 2017; IEEE: Piscataway, NJ, USA, 2018; pp. 1–5.
4. Shah, R.; Goli, P.; Shireen, W. Adaptive Protection Scheme for a Microgrid with High Levels of Renewable Energy Generation. In Proceedings of the 2018 Clemson University Power Systems Conference (PSC), Charleston, SC, USA, 4–7 September 2018; IEEE: Piscataway, NJ, USA, 2019; pp. 1–7.
5. Gomes, M.; Coelho, P.; Moreira, C. Microgrid protection schemes. In *Microgrids Design and Implementation*; Zambroni de Souza, A.C., Castilla, M., Eds.; Springer International Publishing: Cham, Switzerland, 2019; pp. 311–336, ISBN 978-3-319-98686-9.
6. Lotfi-fard, S.; Faiz, J.; Iravani, R. Improved overcurrent protection using symmetrical components. *IEEE Trans. Power Deliv.* **2007**, *22*, 843–850. [CrossRef]
7. Wang, X.; Li, Y.; Yu, Y. Research on the relay protection system for a small laboratory-scale microgrid system. In Proceedings of the 2011 6th IEEE Conference on Industrial Electronics and Applications, Beijing, China, 21–23 June 2011; IEEE: Piscataway, NJ, USA, 2011; pp. 2712–2716.
8. Rockefeller, G.D.; Wagner, C.L.; Linders, J.R.; Hicks, K.L.; Rizy, D.T. Adaptive transmission relaying concepts for improved performance. *IEEE Trans. Power Deliv.* **1988**, *3*, 1446–1458. [CrossRef]
9. Prasai, A.; Du, Y.; Paquette, A.; Buck, E.; Harley, R.; Divan, D. Protection of meshed microgrids with communication overlay. In Proceedings of the 2010 IEEE Energy Conversion Congress and Exposition, Atlanta, GA, USA, 12–16 September 2010; IEEE: Piscataway, NJ, USA, 2011; pp. 64–71.
10. International Electrotechnical Commission. Communication Networks and Systems for Power Utility Automation—Part 3: General Requirements. (IEC 61850-3:2013). 2013. Available online: https://webstore.iec.ch/publication/6010 (accessed on 15 May 2020).
11. Ustun, T.S.; Ozansoy, C.; Zayegh, A. Modeling of a centralized microgrid protection system and distributed energy resources according to IEC 61850-7-420. *IEEE Trans. Power Syst.* **2012**, *27*, 1560–1567. [CrossRef]
12. Ustun, T.S.; Ozansoy, C.; Zayegh, A. A microgrid protection system with central protection unit and extensive communication. In Proceedings of the 2011 10th International Conference on Environment and Electrical Engineering, Rome, Italy, 8–11 May 2011; IEEE: Piscataway, NJ, USA, 2011; pp. 1–4.
13. Chaitanya, B.K.; Soni, A.K.; Yadav, A. Communication assisted fuzzy based adaptive protective relaying scheme for Microgrid. *J. Power Technol.* **2018**, *98*, 57–69.
14. Lin, H.; Guerrero, J.M.; Jia, C.; Tan, Z.-H.; Vasquez, J.C.; Liu, C. Adaptive overcurrent protection for microgrids in extensive distribution systems. In Proceedings of the IECON 2016—42nd Annual Conference of the IEEE Industrial Electronics Society, Florence, Italy, 23–26 October 2016; IEEE: Piscataway, NJ, USA, 2016; pp. 4042–4047.
15. Bapeswara Rao, V.V.; Sankara Rao, K. Computer aided coordination of directional relays: Determination of break points. *IEEE Trans. Power Deliv.* **1988**, *3*, 545–548. [CrossRef]
16. Jenkins, L.; Khincha, H.P.; Shivakumar, S.; Dash, P.K. An application of functional dependencies to the topological analysis of protection schemes. *IEEE Trans. Power Deliv.* **1992**, *7*, 77–83. [CrossRef]
17. Zhu, X. Computational intelligence techniques and applications. In *Computational Intelligence Techniques in Earth and Environmental Sciences*; Islam, T., Srivastava, P.K., Gupta, M., Zhu, X., Mukherjee, S., Eds.; Springer: Dordrecht, The Netherlands, 2014; pp. 3–26, ISBN 978-94-017-8641-6.
18. Yang, X.-S. Chapter 1—Introduction to Algorithms. In *Nature-Inspired Optimization Algorithms*, 1st ed.; Elsevier: Amsterdam, The Netherlands; Boston, MA, USA, 2014; ISBN 978-0-12-416743-8.

19. El-Khattam, W.; Sidhu, T.S. Restoration of directional overcurrent relay coordination in distributed generation systems utilizing fault current limiter. *IEEE Trans. Power Deliv.* **2008**, *23*, 576–585. [CrossRef]
20. Bedekar, P.P.; Bhide, S.R.; Kale, V.S. Optimum coordination of overcurrent relays in distribution system using genetic algorithm. In Proceedings of the 2009 International Conference on Power Systems, Kharagpur, India, 27–29 December 2009; IEEE: Piscataway, NJ, USA, 2010; pp. 1–6.
21. Thangaraj, R.; Pant, M.; Deep, K. Optimal coordination of over-current relays using modified differential evolution algorithms. *Eng. Appl. Artif. Intell.* **2010**, *23*, 820–829. [CrossRef]
22. Najy, W.K.A.; Zeineldin, H.H.; Woon, W.L. Optimal protection coordination for microgrids with grid-connected and islanded capability. *IEEE Trans. Ind. Electron.* **2013**, *60*, 1668–1677. [CrossRef]
23. Shrivastava, A.; Tripathi, J.M.; Krishan, R.; Parida, S.K. Optimal coordination of overcurrent relays using gravitational search algorithm with DG penetration. *IEEE Trans. Ind. Appl.* **2017**. [CrossRef]
24. Abdelsalam, M.; Diab, H.Y. Diab optimal coordination of DOC relays incorporated into a distributed generation-based micro-grid using a meta-heuristic MVO algorithm. *Energies* **2019**, *12*, 4115. [CrossRef]
25. International Electrotechnical Commission. Measuring Relays and Protection Equipment—Part 151: Functional Requirements for Over/Under Current Protection. (IEC 60255-151:2009 ED1). 2009. Available online: https://webstore.iec.ch/publication/1166 (accessed on 15 May 2020).
26. Kapil, S.; Chawla, M. Performance evaluation of K-means clustering algorithm with various distance metrics. In Proceedings of the 2016 IEEE 1st International Conference on Power Electronics, Intelligent Control and Energy Systems (ICPEICES), Delhi, India, 4–6 July 2016; IEEE: Piscataway, NJ, USA, 2017; pp. 1–4.
27. Wadood, A.; Khurshaid, T.; Farkoush, S.G.; Yu, J.; Kim, C.H.; Rhee, S.B. Rhee nature-inspired whale optimization algorithm for optimal coordination of directional overcurrent relays in power systems. *Energies* **2019**, *12*, 2297. [CrossRef]
28. Bouchekara, H.R.E.H.; Zellagui, M.; Abido, M.A. Optimal coordination of directional overcurrent relays using a modified electromagnetic field optimization algorithm. *Appl. Soft Comput.* **2017**, *54*, 267–283. [CrossRef]
29. Bedekar, P.P.; Bhide, S.R. Optimum coordination of directional overcurrent relays using the Hybrid GA-NLP approach. *IEEE Trans. Power Deliv.* **2011**, *26*, 109–119. [CrossRef]
30. Amraee, T. Coordination of directional overcurrent relays using seeker algorithm. *IEEE Trans. Power Deliv.* **2012**, *27*, 1415–1422. [CrossRef]
31. Singh, M.; Panigrahi, B.K.; Abhyankar, A.R.; Das, S. Optimal coordination of directional over-current relays using informative differential evolution algorithm. *J. Comput. Sci.* **2014**, *5*, 269–276. [CrossRef]
32. Birla, D.; Maheshwari, R.P.; Gupta, H.O. A new nonlinear directional overcurrent relay coordination technique, and banes and boons of near-end faults based approach. *IEEE Trans. Power Deliv.* **2006**, *21*, 1176–1182. [CrossRef]
33. Zellagui, M.; Hassan, H. A Hybrid optimization algorithm (IA-PSO) for optimal coordination of directional overcurrent relays in meshed power systems. *WSEAS Trans. Power Syst.* **2015**, *10*, 240–250.
34. Alam, M.N.; Das, B.; Pant, V. An interior point method based protection coordination scheme for directional overcurrent relays in meshed networks. *Int. J. Electr. Power Energy Syst.* **2016**, *81*, 153–164. [CrossRef]
35. Mousavi Motlagh, S.H.; Mazlumi, K. Optimal overcurrent relay coordination using optimized objective function. *ISRN Power Eng.* **2014**, *2014*, 869617. [CrossRef]
36. Senarathna, T.S.S.; Boralessa, M.A.K.S.; Udayanga Hemapala, K.T.M. Effect of the different objective function formulations on DOCR setting optimization. In Proceedings of the 2019 IEEE R10 Humanitarian Technology Conference (R10-HTC) (47129), Depok, West Java, Indonesia, 12–14 November 2019; IEEE: Piscataway, NJ, USA, 2020; pp. 80–85.
37. Wadood, A.; Gholami Farkoush, S.; Khurshaid, T.; Kim, C.-H.; Yu, J.; Geem, Z.; Rhee, S.-B. An optimized protection coordination scheme for the optimal coordination of overcurrent relays using a nature-inspired root tree algorithm. *Appl. Sci.* **2018**, *8*, 1664. [CrossRef]
38. Darji, G.; Patel, A.; Mehta, R.P. Optimal coordination of directional overcurrent relays using AI algorithms and comparison. *Kalpa Pub. Eng.* **2017**, *1*, 81–89. [CrossRef]
39. Yang, X.-S. Chapter 14—Multi-objective optimization. In *Nature-Inspired Optimization Algorithms*, 1st ed.; Elsevier: Amsterdam, The Netherlands; Boston, MA, USA, 2014; ISBN 978-0-12-416743-8.
40. Gutierrez, E.H.; Conde, A.; Shih, M.Y.; Fernández, E. Execution time enhancement of DOCR coordination algorithms for on-line application. *Electr. Power Syst. Res.* **2019**, *170*, 1–12. [CrossRef]

41. University of Washington. *Power Systems Test Case Archive*; University of Washington: Seattle, WA, USA. Available online: http://labs.ece.uw.edu/pstca/pf14/pg_tca14bus.htm (accessed on 15 December 2019).
42. International Electrotechnical Commission. *Short-Circuit Currents in Three-Phase a.c. Systems—Part 0: Calculation of Currents*; (IEC 60909-0:2016); 2016. Available online: https://webstore.iec.ch/publication/24100 (accessed on 15 May 2020).
43. Boutsika, T.N.; Papathanassiou, S.A. Short-circuit calculations in networks with distributed generation. *Electr. Power Syst. Res.* **2008**, *78*, 1181–1191. [CrossRef]
44. Gers, J.M.; Holmes, E.J. *Protection of Electricity Distribution Networks*, 2nd ed.; IEE Power & Energy Series 47; Institution of Engineering and Technology: London, UK, 2004.
45. Khalilpourazari, S.; Khalilpourazary, S. An efficient hybrid algorithm based on water cycle and moth-flame optimization algorithms for solving numerical and constrained engineering optimization problems. *Soft Comput.* **2019**, *23*, 1699–1722. [CrossRef]
46. Masuda, K.; Kurihara, K.; Aiyoshi, E. A penalty approach to handle inequality constraints in particle swarm optimization. In Proceedings of the 2010 IEEE International Conference on Systems, Man and Cybernetics, Istanbul, Turkey, 10–13 October 2010; IEEE: Piscataway, NJ, USA, 2010; pp. 2520–2525.
47. Mansour, M.M.; Mekhamer, S.F.; El-Kharbawe, N. A modified particle swarm optimizer for the coordination of directional overcurrent relays. *IEEE Trans. Power Deliv.* **2007**, *22*, 1400–1410. [CrossRef]
48. Mirjalili, S.; Hashim, S.Z.M. A new hybrid PSOGSA algorithm for function optimization. In Proceedings of the 2010 International Conference on Computer and Information Application, Tianjin, China, 3–5 December 2010; IEEE: Piscataway, NJ, USA, 2012; pp. 374–377.
49. Srivastava, A.; Tripathi, J.M.; Mohanty, S.R.; Panda, B. Optimal over-current relay coordination with distributed generation using hybrid particle swarm optimization–gravitational search algorithm. *Electr. Power Compon. Syst.* **2016**, *44*, 506–517. [CrossRef]
50. Heidari, A.A.; Mirjalili, S.; Faris, H.; Aljarah, I.; Mafarja, M.; Chen, H. Harris hawks optimization: Algorithm and applications. *Future Gener. Comput. Syst.* **2019**, *97*, 849–872. [CrossRef]
51. Yu, J.; Kim, C.-H.; Rhee, S.-B. The comparison of lately proposed Harris hawks optimization and jaya optimization in solving directional overcurrent relays coordination problem. *Complexity* **2020**, *2020*, 3807653. [CrossRef]
52. Mirjalili, S.; Lewis, A. The whale optimization algorithm. *Adv. Eng. Softw.* **2016**, *95*, 51–67. [CrossRef]
53. Mirjalili, S.; Mirjalili, S.M.; Lewis, A. Grey wolf optimizer. *Adv. Eng. Softw.* **2014**, *69*, 46–61. [CrossRef]
54. Korashy, A.; Kamel, S.; Youssef, A.-R.; Jurado, F. Solving optimal coordination of direction overcurrent relays problem using grey wolf optimization (GWO) algorithm. In Proceedings of the 2018 Twentieth International Middle East Power Systems Conference (MEPCON), Cairo, Egypt, 18–20 December 2018; IEEE: Piscataway, NJ, USA, 2019; pp. 621–625.